AIP | Applied Physics Letters

Analysis of InGaN-delta-InN quantum wells for light-emitting diodes

Hongping Zhao, Guangyu Liu, and Nelson Tansu

Citation: Appl. Phys. Lett. **97**, 131114 (2010); doi: 10.1063/1.3493188
View online: http://dx.doi.org/10.1063/1.3493188
View Table of Contents: http://apl.aip.org/resource/1/APPLAB/v97/i13
Published by the American Institute of Physics.

Analysis of InGaN-delta-InN quantum wells for light-emitting diodes

Hongping Zhao,[a] Guangyu Liu, and Nelson Tansu[b]
Department of Electrical and Computer Engineering, Center for Optical Technologies, Lehigh University, Bethlehem, Pennsylvania 18015, USA

(Received 5 July 2010; accepted 5 September 2010; published online 1 October 2010)

The design of InGaN-delta-InN quantum wells (QWs) leads to significant redshift for nitride active region with large electron-hole wave function overlap (Γ_{e_hh}) and spontaneous emission rate. The analysis was carried out by using self-consistent six-band $k\cdot p$ band formalism. The design of active region consisting of 30 Å $In_{0.25}Ga_{0.75}N$ QW with InN delta-layer leads to large Γ_{e_hh} of >50% with emission wavelength in the yellow and red spectral regimes, which is applicable for nitride-based light-emitting diodes. © *2010 American Institute of Physics*. [doi:10.1063/1.3493188]

High-efficiency InGaN quantum wells (QWs) light-emitting diodes (LEDs) play an important role in solid-state lighting and display applications.[1–3] Due to the polarization fields in InGaN QW, the electron and hole wave functions are confined in opposite directions leading to reduction of the electron-hole wave function overlap (Γ_{e_hh}). The detrimental effect from charge separation becomes more severe, as the emission wavelength of the InGaN QWs is extended into green and red spectral regimes. Several approaches have been proposed to address the charge separation in InGaN QW as follow: nonpolar InGaN QW,[4] InGaN QW with AlGaN δ-layer,[5,6] staggered InGaN QW,[7–15] type-II InGaN-based QW,[16–18] and strain-compensated InGaN QW.[19]

Recently, the use of staggered InGaN QWs with enhanced matrix element results in increase in radiative recombination rate and radiative efficiency for nitride LEDs.[7–13] Despite its larger overlap Γ_{e_hh} over conventional QW (Γ_{e_hh}=37% for $\lambda\sim$420 nm; Γ_{e_hh}=17% for $\lambda\sim$500 nm), the optimized Γ_{e_hh} for staggered InGaN QW decreases (Γ_{e_hh}=68% for $\lambda\sim$420 nm; Γ_{e_hh}=32% for $\lambda\sim$500 nm)[8,9,12] as its emission wavelength extends to longer spectral regime.

In this work, we present a nitride-based active region with high Γ_{e_hh} by employing InGaN-delta-InN QW. The insertion of ultrathin layer (3–6 Å) of narrow-band gap InN alloy (E_g=0.69 eV) in InGaN QW leads to significant enhancement of Γ_{e_hh}. In contrast to the existing approaches to enhance the overlap,[5–19] the optimized Γ_{e_hh} for the InGaN-delta-InN QW increases as its emission wavelength extends to longer spectral regimes. The optical properties of InGaN-delta-InN QW are compared to those of the conventional InGaN QW for LEDs.

The calculation of the band structures and wave functions for InGaN-based QWs with GaN barriers is based on a self-consistent six-band $k\cdot p$ formalism.[19–23] The details of the numerical model were presented in Ref. 19, and all the computation parameters were obtained from Refs. 24 and 25. In this calculation, all possible transitions between the confined states of the conduction bands and valence bands are taken into account.

To illustrate the challenging issue to redshift the emission wavelength in InGaN QWs, Fig. 1 plots the Γ_{e_hh} (left) and peak emission wavelength (right) as a function of the indium (In) content for InGaN QW with QW thicknesses (d_{QW}) of d_{QW}=2 nm and d_{QW}=3 nm. As the In-content increases from 5% to 45%, the Γ_{e_hh} decreases from 60% (47%) to 27.8% (6.8%) while the emission wavelength increases from 372 nm (377 nm) to 640 nm (871 nm) for the InGaN QW with d_{QW}=2 nm (d_{QW}=3 nm). Similarly, when the d_{QW} increases, the emission wavelength extends longer while the Γ_{e_hh} decreases significantly. Thus, it is important to employ QW designs with enhanced $\Gamma_{e\text{-}hh}$, as the emission wavelength is redshifted.

Figures 2(a) and 2(b) show the energy band lineup profiles and the wave functions of the first conduction subband (C1) and the first valence subband (HH1) at zone center for (a) conventional 30 Å $In_{0.25}Ga_{0.75}N$ QW and (b) 30 Å $In_{0.25}Ga_{0.75}N$ QW with inserted 3 Å InN delta-layer. Due to the existence of the internal electric filed, the charge separation leads to a significant reduction in Γ_{e_hh} of 14.8% for conventional 30 Å $In_{0.25}Ga_{0.75}N$ QW with emission wavelength of 492 nm. By inserting 3 Å InN delta-layer in the center of the 30 Å $In_{0.25}Ga_{0.75}N$ QW [Fig. 2(b)], the large band offset between InGaN and InN leads to the strong localization of electron and hole wave functions toward the center for the QW resulting in enhanced Γ_{e_hh} of 29%. The introduction of the InN delta-layer in the InGaN QW leads to strong modification of the electron and hole wave functions resulting in significant increase in the Γ_{e_hh}, as well as accompanied by a strong redshift of the transition wavelength up to 590 nm. Thus, the InGaN-delta-InN QW is conceptu-

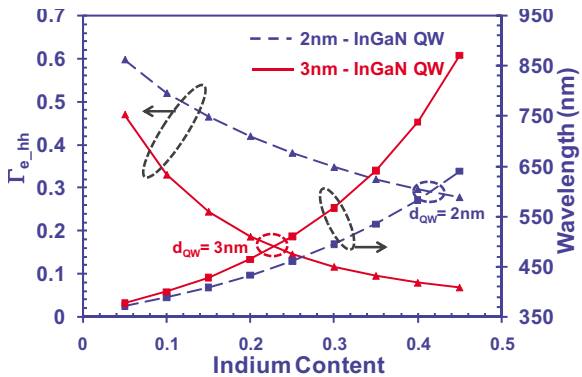

FIG. 1. (Color online) Electron-hole wave function overlap (Γ_{e_hh}) (left) and peak emission wavelength (right) vs indium content with InGaN QW thickness (d_{QW}) of d_{QW}=2 nm and d_{QW}=3 nm.

[a]Electronic mail: hoz207@lehigh.edu.
[b]Electronic mail: tansu@lehigh.edu.

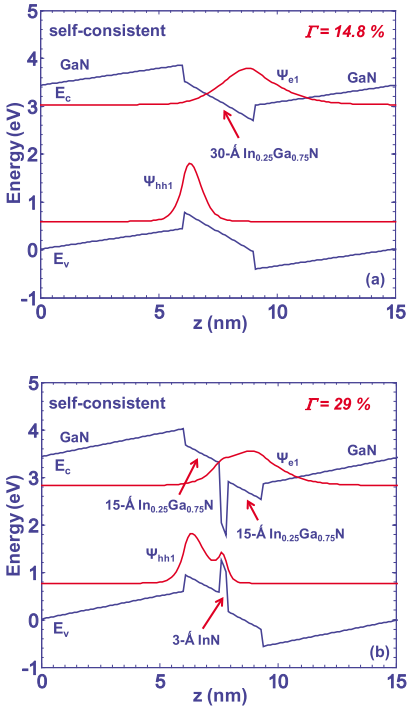

FIG. 2. (Color online) Energy band lineups of (a) conventional 30 Å $In_{0.25}Ga_{0.75}N$ QW, and (b) 30 Å $In_{0.25}Ga_{0.75}N$/3 Å InN QW with electron wave function of EC1 and hole wave function of HH1.

ally very distinct from the three-layer staggered InGaN QW,[9–12] where the latter overlap Γ_{e_hh} decreases as the emission wavelength extends to the longer spectral regime.

Recently, Che *et al.*[26] have proposed the use of asymmetric GaN/InN/InGaN/GaN QWs structure with InN monolayer thickness, which leads to increase in Γ_{e_hh} from the introduction of ultrathin InN layer resulting in strong localization of electron and hole wave functions in the InN/InGaN

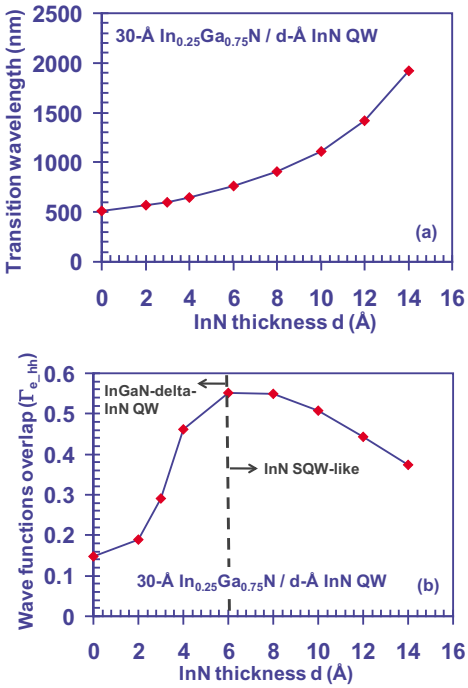

FIG. 3. (Color online) (a) Interband transition wavelength and (b) electron-hole wave function overlap (Γ_{e_hh}) vs InN layer thickness for 30 Å $In_{0.25}Ga_{0.75}N$/d Å InN QW for both cases of InGaN-delta-InN QW (d<6 Å) and InN SQW-like (d>6 Å).

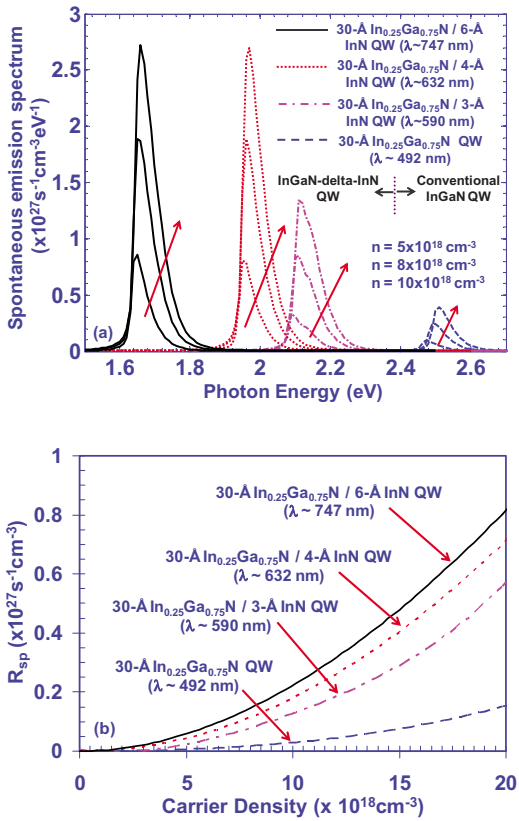

FIG. 4. (Color online) (a) Spontaneous emission spectra for conventional 30 Å $In_{0.25}Ga_{0.75}N$ QW, 30 Å $In_{0.25}Ga_{0.75}N$/3 Å InN QW, 30 Å $In_{0.25}Ga_{0.75}N$/4 Å InN QW and 30 Å $In_{0.25}Ga_{0.75}N$/6 Å InN QW with carrier density $n=5\times10^{18}-10\times10^{18}$ cm^{-3}, and (b) spontaneous emission radiative recombination rate (R_{sp}) as a function of carrier density up to 20 $\times10^{18}$ cm^{-3} for the three QW structures at T=300 K.

interface. In contrast to the asymmetric QWs,[26] our approach focused on the insertion of InN delta-layer in the center of InGaN QW, which leads to strong localization of electron and hole wave functions toward the center for the QW.

Figure 3(a) shows the interband transition wavelength versus the thickness (d Å) of the InN layer for 30 Å $In_{0.25}Ga_{0.75}N$/d Å InN QW structure. The interband transition wavelength increases as the thickness of the InN layer increases. Figure 3(b) shows the overlap (Γ_{e_hh}) versus the thickness (d Å) of the InN layer for 30 Å $In_{0.25}Ga_{0.75}N$/d Å InN QW structure. When the InN layer thickness is ≤6 Å (as delta layer), the Γ_{e_hh} increases as InN layer thickness increases due to the shift of the electron and hole wave functions toward the center of the InGaN QW. Note that the design of InGaN QW with delta-InN layer (<6 Å) allows one to redshift the emission wavelength significantly accompanied by enhancement in the Γ_{e_hh}. Thus, the role of the InN layer in the InGaN-delta-InN QW structure is very different from that in the InN single quantum well (SQW) [Fig. 3(b)]. When the InN layer thickness is >6 Å, the Γ_{e_hh} reduces as InN layer thickness increases, which indicates that the InN layer behaves as SQW.

Figure 4(a) shows the spontaneous emission spectra for conventional 30 Å $In_{0.25}Ga_{0.75}N$ QW (dash line), 30 Å $In_{0.25}Ga_{0.75}N$/3 Å InN QW (dashed-dotted line), 30 Å $In_{0.25}Ga_{0.75}N$/4 Å InN QW (dotted-dotted line) and 30 Å $In_{0.25}Ga_{0.75}N$/6 Å InN QW (solid line) at carrier densities (n) of $n=5\times10^{18}-10\times10^{18}$ cm^{-3} at T=300 K. From the insertion of InN delta-layer, the transition wavelength shows

significant redshift as compared to that of the conventional InGaN QW. The 30 Å $In_{0.25}Ga_{0.75}N/3$ Å InN QW shows a redshift from 492 nm (conventional InGaN QW) to 590 nm with ~3.4 times higher of the peak spontaneous emission spectra (1.34×10^{27} s^{-1} cm^{-3} eV^{-1}) than that of the conventional one (3.9×10^{26} s^{-1} cm^{-3} eV^{-1}) at $n=10\times10^{18}$ cm^{-3}. The $In_{0.25}Ga_{0.75}N$ QW with 6 Å InN delta-layer shows a redshift from 492 nm (conventional InGaN QW) to 747 nm with ~7 times higher of the peak spontaneous emission spectra (2.73×10^{27} s^{-1} cm^{-3} eV^{-1}) than that of the conventional one at $n=10\times10^{18}$ cm^{-3}.

Figure 4(b) illustrates the spontaneous emission radiative recombination rate per unit volume (R_{sp}) for conventional 30 Å $In_{0.25}Ga_{0.75}N$ QW, 30 Å $In_{0.25}Ga_{0.75}N/3$ Å InN QW, 30 Å $In_{0.25}Ga_{0.75}N/4$ Å InN QW, and 30 Å $In_{0.25}Ga_{0.75}N/6$ Å InN QW as a function of carrier density. For the 30 Å $In_{0.25}Ga_{0.75}N/3$ Å InN QW structure, the R_{sp} is enhanced by 4–4.6 times at each carrier density as compared to that for conventional 30 Å $In_{0.25}Ga_{0.75}N$ QW. The enhancement of the R_{sp} for the 30 Å $In_{0.25}Ga_{0.75}N/4$ Å (6 Å) InN QW ranges between 5.2–8.3 (6.4–12) times.

Note that high quality InN alloy have been reported for material grown by metal organic chemical vapor deposition (MOCVD) (Refs. 27–33) and molecular beam epitaxy (MBE).[26,33–37] The growths of InN material by MBE have resulted in high electron mobility in the order of 2370 $cm^2/(V\,s)$.[34] The use of pulsed MOCVD has also resulted in high optical quality InN alloy.[27,28] Recent experimental studies by MBE have also indicated the capabilities to grow InN with monolayer precision.[26,37]

The key idea from this work is to illustrate the advantage arises from the insertion of narrow-band gap delta-layer in InGaN QW, which enables the extension of emission wavelength while resulting in QW with large matrix element and large radiative recombination rate. Experimental studies are required to clarify on the optimized design for realistic InGaN-delta-InN QW LEDs, which require the need to take into account the large lattice mismatch and phase separation issues in InN/InGaN heterostructure, as well as current injection efficiency in nitride LEDs.[38]

Our analysis assumes that the InN delta-layer inserted in InGaN QW as uniform ultrathin layer, thus the active region is treated as two-dimensional QW structure. However, the InN nonuniformity or clustering may lead to quantum-dot like characteristics, which will require further investigation. However, it is important to point out that the challenges in the high precision control in the epitaxy of very thin InN layer may present potential advantage, in particular for realizing broadband white emission from the potential thickness variation or InN clustering from the InN delta-layer.

In summary, the design of delta-InN layer inserted in the InGaN QW results in the ability to extend its emission wavelength into yellow and red spectral regime, with significantly enhanced matrix element and spontaneous emission rate. The design of 30 Å InGaN QW with 3 Å (6 Å) InN delta-layer shows redshift in the emission wavelength by ~100 nm (~250 nm) with enhancement of the spontaneous emission rate of ~4–4.6 times (~6.4–12 times) as compared to that of the conventional InGaN QW. The InGaN-delta-InN QW has potential for achieving high-efficiency nitride LEDs and lasers emitting in the yellow and red spectral regime.

This work is supported by Department of Energy (DE-FC26-08NT01581), National Science Foundation (ECCS 0701421), and Class of 1961 Professorship Fund.

[1]N. Tansu, H. Zhao, G. Liu, X. H. Li, J. Zhang, H. Tong, and Y. K. Ee, IEEE Photonics J. **2**, 236 (2010).
[2]M. H. Kim, M. F. Schubert, Q. Dai, J. K. Kim, E. F. Schubert, J. Piprek, and Y. Park, Appl. Phys. Lett. **91**, 183507 (2007).
[3]Y. K. Ee, P. Kumnorkaew, R. A. Arif, H. Tong, H. Zhao, J. F. Gilchrist, and N. Tansu, IEEE J. Sel. Top. Quantum Electron. **15**, 1218 (2009).
[4]R. M. Farrell, D. F. Feezell, M. C. Schmidt, D. A. Haeger, K. M. Kelchner, K. Iso, H. Yamada, M. Saito, K. Fujito, D. A. Cohen, J. S. Speck, S. P. DenBaars, and S. Nakamura, Jpn. J. Appl. Phys., Part 2 **46**, L761 (2007).
[5]J. Park and Y. Kawakami, Appl. Phys. Lett. **88**, 202107 (2006).
[6]S. H. Park, J. Park, and E. Yoon, Appl. Phys. Lett. **90**, 023508 (2007).
[7]R. A. Arif, Y. K. Ee, and N. Tansu, Appl. Phys. Lett. **91**, 091110 (2007).
[8]R. A. Arif, H. Zhao, and N. Tansu, IEEE J. Quantum Electron. **44**, 573 (2008).
[9]H. Zhao, R. A. Arif, and N. Tansu, IEEE J. Sel. Top. Quantum Electron. **15**, 1104 (2009).
[10]H. Zhao, G. S. Huang, G. Liu, X. H. Li, J. D. Poplawsky, S. Tafon Penn, V. Dierolf, and N. Tansu, Appl. Phys. Lett. **95**, 061104 (2009).
[11]H. P. Zhao, G. Y. Liu, X. H. Li, R. A. Arif, G. S. Huang, J. D. Poplawsky, S. Tafon Penn, V. Dierolf, and N. Tansu, IET Optoelectron. **3**, 283 (2009).
[12]H. Zhao and N. Tansu, J. Appl. Phys. **107**, 113110 (2010).
[13]S. H. Park, D. Ahn, and J. W. Kim, Appl. Phys. Lett. **94**, 041109 (2009).
[14]S. H. Park, D. Ahn, B. H. Koo, and J. W. Kim, Appl. Phys. Lett. **95**, 063507 (2009).
[15]S. H. Yen and Y. K. Kuo, Opt. Commun. **281**, 4735 (2008).
[16]R. A. Arif, H. Zhao, and N. Tansu, Appl. Phys. Lett. **92**, 011104 (2008).
[17]H. Zhao, R. A. Arif, and N. Tansu, J. Appl. Phys. **104**, 043104 (2008).
[18]S. H. Park, D. Ahn, B. H. Koo, and J. E. Oh, Appl. Phys. Lett. **96**, 051106 (2010).
[19]H. Zhao, R. A. Arif, Y. K. Ee, and N. Tansu, IEEE J. Quantum Electron. **45**, 66 (2009).
[20]S. L. Chuang and C. S. Chang, Phys. Rev. B **54**, 2491 (1996).
[21]S. L. Chuang, IEEE J. Quantum Electron. **32**, 1791 (1996).
[22]S. L. Chuang and C. S. Chang, Semicond. Sci. Technol. **12**, 252 (1997).
[23]S. L. Chuang, *Physics of Photonic Devices*, 2nd ed. (Wiley, New York, 2009), Chap. 4.
[24]I. Vurgaftman and J. R. Meyer, in *Nitride Semiconductor Devices*, edited by J. Piprek (Wiley, New York, 2007), Chap. 2.
[25]I. Vurgaftman and J. R. Meyer, J. Appl. Phys. **94**, 3675 (2003).
[26]S. Che, A. Yuki, H. Watanabe, Y. Ishitani, and A. Yoshikawa, Appl. Phys. Express **2**, 021001 (2009).
[27]M. Jamil, H. Zhao, J. Higgins, and N. Tansu, J. Cryst. Growth **310**, 4947 (2008).
[28]M. Jamil, H. Zhao, J. Higgins, and N. Tansu, Phys. Status Solidi A **205**, 2886 (2008).
[29]M. Jamil, R. A. Arif, Y. K. Ee, H. Tong, J. B. Higgins, and N. Tansu, Phys. Status Solidi A **205**, 1619 (2008).
[30]M. Alevli, G. Durkaya, A. Weerasekara, A. G. U. Perera, N. Dietz, W. Fenwick, V. Woods, and I. Ferguson, Appl. Phys. Lett. **89**, 112119 (2006).
[31]N. Khan, A. Sedhain, J. Li, J. Y. Lin, and H. X. Jiang, Appl. Phys. Lett. **92**, 172101 (2008).
[32]A. Kadir, T. Ganguli, M. R. Gokhale, A. P. Shah, S. S. Chandvankar, B. M. Arora, and A. Bhattacharya, J. Cryst. Growth **298**, 403 (2007).
[33]G. Xu, Y. J. Ding, H. P. Zhao, M. Jamil, G. Y. Liu, N. Tansu, I. B. Zotova, C. E. Stutz, D. E. Diggs, N. Fernelius, F. K. Hopkins, C. S. Gallinat, G. Koblmüller, and J. S. Speck, Semicond. Sci. Technol. **25**, 015004 (2010).
[34]G. Koblmüller, C. S. Gallinat, S. Bernardis, J. S. Speck, G. D. Chern, E. D. Readinger, H. Shen, and M. Wraback, Appl. Phys. Lett. **89**, 071902 (2006).
[35]K. Wang, T. Kosel, and D. Jena, Phys. Status Solidi C **5**, 1811 (2008).
[36]J. Wu, W. Walukiewicz, K. M. Yu, W. Shan, J. W. Ager III, E. E. Haller, A. Hai Lu, W. J. Schaff, W. K. Metzger, and S. Kurtz, J. Appl. Phys. **94**, 6477 (2003).
[37]A. Yuki, H. Watanabe, S. B. Che, Y. Ishitani, and A. Yoshikawa, Phys. Status Solidi C **6**, S417 (2009).
[38]H. Zhao, G. Liu, R. A. Arif, and N. Tansu, Solid-State Electron. **54**, 1119 (2010).